Non-peer-reviewed EarthArXiv preprint; submitted to Remote Sensing of Environment *(Elsevier).*

Land subsidence in Jakarta in Three Dimensions (2014–2025) using InSAR–GNSS Datum Connection and the Strapdown Decomposition

Alexandru M. Lapadat[a,*], Heri Andreas[b], Wietske S. Brouwer[a], Simon A.N. van Diepen[a], Dhota Pradipta[b], Ramon F. Hanssen[a]

[a] *Mathematical Geodesy and Positioning, Delft University of Technology, Stevinweg 1, Delft, Netherlands*
[b] *Geodesy Research Division, Institute of Technology Bandung, Jl. Ganesha 10, Bandung, Indonesia*

Abstract

Coastal megacities face compounding hazards from rising sea levels and land subsidence. Jakarta, one of the fastest-sinking megacities, already experiences recurrent flooding amplified by rapid land subsidence. Assessing and mitigating this hazard requires reliable estimates of three-dimensional ground motion over wide spatial and temporal scales in a well-defined geodetic reference frame and datum. Here we combine spaceborne InSAR and GNSS measurements. We develop a datum connection procedure that aligns multi-track InSAR line-of-sight datasets between 2014 and 2025 to a common datum for unbiased three-dimensional velocity decomposition, and connect the resulting displacement field to the Sunda plate-fixed frame using GNSS, yielding a 3D characterization of Jakarta's land deformation in a globally consistent reference frame. Our results show that Jakarta's land motion is dominated by six main subsidence bowls, with subsidence and directional horizontal rates of up to -7.7 cm/yr and 1.7 cm/yr, respectively, overlying slow regional subsidence of -1.1 cm/yr across the metropolitan area. As these results hinge on the availability of one single continuous GNSS station, we recommend the installation of dedicated geodetic ground-based infrastructure to ensure sustainable and rigorous monitoring capabilities for the future.

*Corresponding author
Email address: A.M.Lapadat@tudelft.nl (Alexandru M. Lapadat)

Keywords: InSAR, GNSS, datum, geodesy, land subsidence, Jakarta

1. Introduction

Jakarta, the world's most populous city with close to 42 million residents (United Nations and Social Affairs, 2025), is among the fastest-sinking megacities on Earth. Historically, using observations since 1925 (Schepers, 1926; Schuitenvoerder, 1926), subsidence occurred at two distinct scales: a citywide north-dipping tilt spanning ∼30 km[1], with rates declining from −4.5 cm/yr in the north to near-zero in the south, and localized subsidence bowls superimposed on this trend, whose extent and intensity vary spatiotemporally, with maximum rates ranging from −7 to −15 cm/yr (Abidin et al., 2001, 2011, 2022). Currently, ∼15% of Jakarta's land area—mainly in the northern districts—already lies below mean sea level, leaving these areas prone to inundation during ordinary high tides (Juliandri et al., 2022). While citywide catastrophic floods in the past decade have been mostly driven by extreme rainfall and river runoff, in North Jakarta it is the subsidence that is causing recurrent tidal flooding, a risk further intensified by ongoing regional sea-level rise (Fenoglio-Marc et al., 2012). Jakarta's subsidence is attributed to three interacting mechanisms: (i) natural compaction of young Quaternary coastal alluvium, (ii) increased effective stress from the load of dense urban development and infrastructure, and (iii) groundwater extraction, which reduces pore pressure in the aquifer system and induces localized, bowl-shaped subsidence (Murdohardono and Sudarsono, 1998; Abidin et al., 2001; Colbran, 2009; Batubara et al., 2023). While natural compaction and loading act gradually, groundwater withdrawal produces rapid and spatially concentrated deformation. The combined effects are structural damage to buildings, cracking and tilting (Abidin et al., 2015; Nugraha et al., 2024), and recurrent flooding (Takagi et al., 2016; Sagala et al., 2013; Firman et al., 2011; Lubis et al., 2022), making land subsidence one of the most critical hazards for Jakarta's long-term sustainability. The combined processes (Abidin et al., 2022; Bennett et al., 2023; Lubis et al., 2022; Colbran, 2009; Takagi et al., 2016; Sagala et al., 2013; Firman et al., 2011) of land subsidence, sea-level rise, extreme precipitation, and runoff put Jakarta at risk, with subsidence amplifying hazards by lowering ground elevation, increasing coastal flood ex-

[1]from Ancol to Pasar Rebo

posure, and accelerating runoff. These impacts make precise estimation and continuous monitoring of land subsidence essential for effective risk assessment and flood mitigation (Abidin et al., 2015).

Over the past four decades, a range of geodetic techniques (Abidin et al., 2004) have been applied, each with distinct strengths and limitations. Spirit leveling in the 1980s (Abidin et al., 2001; Ekkelenkamp, 2019; Schepers, 1926; Schuitenvoerder, 1926) provided millimeter-level precision but was costly, slow, and spatially sparse. Of the 45 benchmarks established in 1982 (Abidin et al., 2001), many have since disappeared due to Jakarta's rapid urban development. GNSS campaigns from the 1990s onward (Abidin et al., 2001, 2008; Abdullah et al., 2021; Susilo et al., 2023) expanded from 13 benchmarks to 65 by 2010, improving spatial coverage and revealing broader subsidence patterns, but in the meantime several benchmarks became unobservable due to monument destruction (Abidin et al., 2011). Thus, for both leveling and GNSS, the loss or inaccessibility of benchmarks limits the temporal continuity and spatial completeness of the subsidence record. The introduction of spaceborne Interferometric Synthetic Aperture Radar (InSAR) (Hanssen, 2001) in the 1990s revolutionized monitoring, offering dense spatial coverage and frequent temporal sampling across Jakarta's metropolitan area (Abidin et al., 2005, 2011). Early InSAR studies (Abidin et al., 2005; Ng et al., 2012; Koudogbo et al., 2012; Chaussard et al., 2013; Widodo et al., 2019) from Jakarta relied on short, single-track SAR datasets and suffered from temporal decorrelation (Zebker and Villasenor, 1992). Advances in processing methods (e.g., Persistent Scatterer Interferometry (PSI) (Ferretti et al., 2002b,a) and Small Baseline Subset (SBAS) (Berardino et al., 2003; Hooper, 2008)) combined with greater computational capacity, have enabled longer time series and multi-track coverage (Hakim et al., 2020; Zhang et al., 2025; Sidiq et al., 2025).

As InSAR observes the projection of the 3D displacement vector onto the radar line of sight (LoS), often these estimates were projected onto the vertical (PoV), an error-free operation only if horizontal displacements are negligible (Brouwer and Hanssen, 2023). Consequently, vertical PoV displacements are biased in localized subsidence bowls. Harintaka et al. (2024) combined ascending and descending tracks to estimate the projection of the displacement onto the East–Up plane, still biased (Brouwer and Hanssen, 2023). Therefore, no InSAR product currently provides a complete three-dimensional view of ground motion in Jakarta.

A second issue is that nearly all InSAR-based velocity maps of Jakarta

are relative, given in a local InSAR datum. The 'null-location', where the displacement rate is 0 mm/yr, is unknown. This rank defect can result in misleading geophysical interpretations, such as apparent uplift in central Jakarta (Widodo et al., 2019; Zhang et al., 2025), which is physically unrealistic. Consequently, studies focusing on fast-subsiding bowls driven by groundwater extraction may overlook slower, widespread regional subsidence, which can be obscured if the InSAR datum is not linked to a plate-fixed reference frame, such as the Sunda plate-fixed frame (Yong et al., 2017).

Here, we introduce an optimization-constrained strapdown decomposition (Brouwer and Hanssen, 2024) that aligns multi-track InSAR data to a common datum and connects InSAR-derived land motion with GNSS to a global reference frame, enabling the first estimation of three-dimensional velocity vectors across Jakarta in the Sunda plate-fixed frame. In Sec. 2 we present the input datasets and the methodology for multi-track InSAR alignment and the datum connection of the InSAR velocity map to the Sunda plate-fixed frame using GNSS. In Sec. 3, we apply the method to two InSAR tracks and produce an intermediary velocity map expressed in a common local InSAR datum. We then estimate the velocity offset between the local InSAR datum and the Sunda plate-fixed frame at the location of a continuously operating GNSS reference station (CORS) and apply this offset to the intermediary velocity map, producing a 3D velocity field for Jakarta in the Sunda plate-fixed frame. Sec. 4 presents the resulting subsidence patterns, and the final section summarizes the key findings and their implications for Jakarta.

2. Methodology

We subsequently discuss the input datasets and the decomposition assumptions, followed by the inter-track datum alignment establishing a common InSAR datum, and a methodology for estimating the motion of this common InSAR datum within the Sunda plate-fixed frame.

2.1. Dataset Preparation

We use two datasets of linear velocities estimated from InSAR Point Scatterer[2] (PS) displacement time series spanning 2014–2025, see Fig. 1. The

[2]We use the Delft taxonomy for scatterer classification, see (Hu et al., 2019)

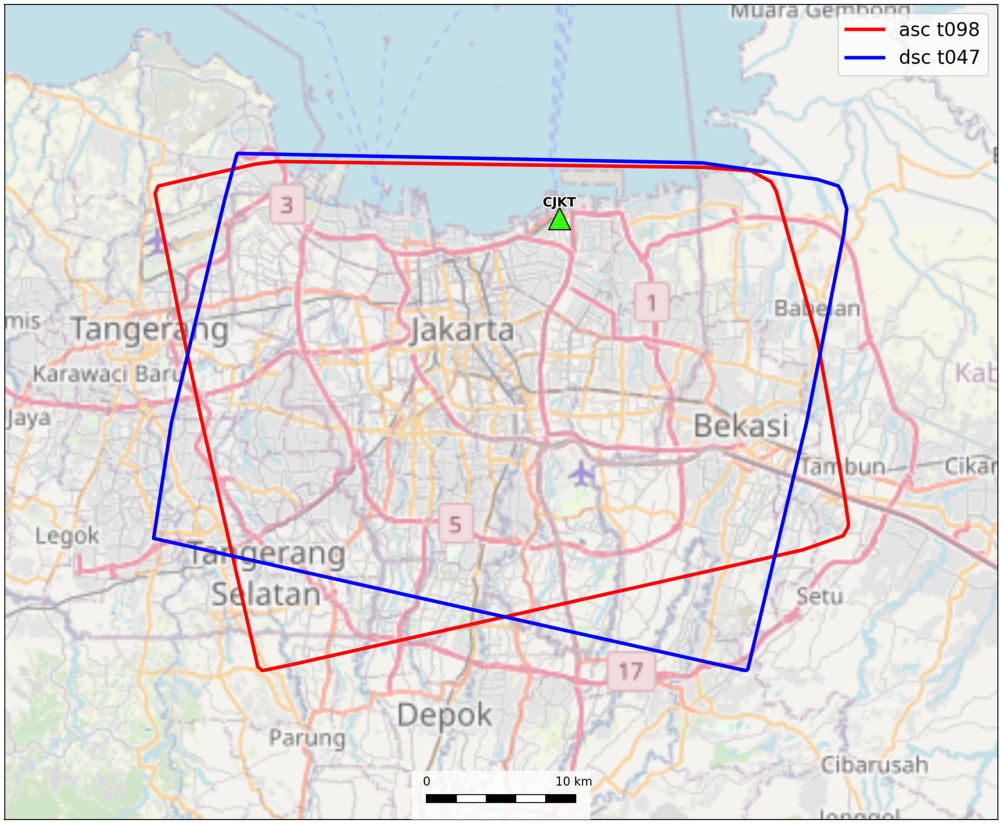

Figure 1: Area of Interest (AOI) covering the Jakarta metropolitan area, showing the Sentinel-1 ascending (track 98, red) and descending (track 47, blue) footprints. The location of the CORS GNSS station CJKT used for datum alignment is indicated as a green triangle.

datasets were generated from 281 Sentinel-1 acquisitions from ascending track 98 and 183 acquisitions from descending track 47, using the Delft implementation of Persistent Scatterer Interferometry, DePSI (Kampes, 2006; Van Leijen, 2014). Each track uses a unique local datum defined by its mean linear velocity. Consequently, all velocities are relative and must be interpreted in terms of the spatial variability.

Additionally, we use GNSS data from station CJKT, see Figs. 1 and 2, a long-term CORS to align the common InSAR datum with the Sunda plate-fixed frame. CJKT is located at Tanjung Priok and operated by Badan Informasi Geospasial (BIG), with its antenna mounted on a 2 m tall cast-concrete pillar on the roof of a two-story building, see Fig. 2b. The daily station

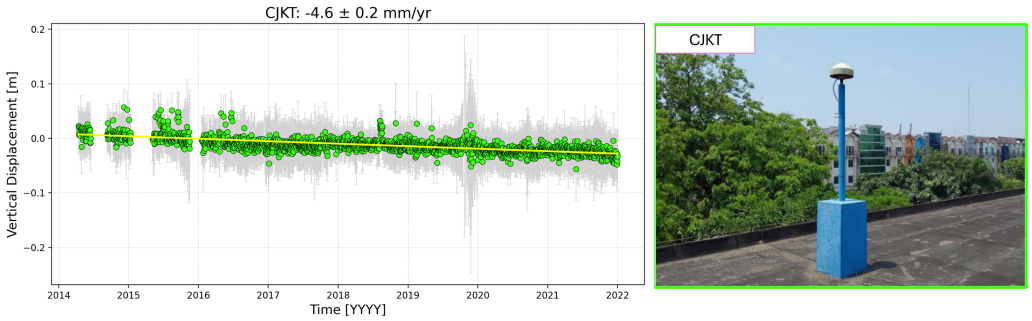

Figure 2: (a) Vertical displacement time series for the CJKT CORS station (green markers) with associated 2σ uncertainties. The yellow line shows the Best Linear Unbiased Estimator (BLUE) least-squares fit for 2014–2022, yielding a velocity of -4.6 ± 0.2 mm/yr. This velocity is used to tie the relative InSAR measurements to the Sunda plate-fixed frame. (b) CJKT station location.

coordinates were derived from continuous GPS phase observations collected between October 2010 and January 2022. The GNSS data were processed by Susilo et al. (2023) in differential mode using the GAMIT/GLOBK software package version 10.71 (Herring et al., 2010). Daily station positions were estimated using double-differenced, ionosphere-free phase observations

with respect to 12 IGS reference stations. This yields station coordinates in ITRF2014, applying precise IGS orbits, atmospheric delay modeling, and standard tidal and loading corrections. The daily solutions were subsequently combined and aligned in GLOBK to the IGb14[3] using eight stable global reference stations.

The vertical displacement time series of CJKT, together with their 2σ uncertainties, see Fig. 2a, were subsampled over 2014–2022 to align with the InSAR observation period and used to estimate linear vertical velocity in the Sunda plate-fixed frame, assuming a constant displacement rate consistent with the approach used for the InSAR data.

2.2. LoS decomposition to 3D velocity

To convert the InSAR LoS velocities into physically meaningful 3D components, we apply the strapdown decomposition method (Brouwer and Hanssen, 2024, 2021), which transforms ascending and descending LoS observations into a local transversal-longitudinal-normal (TLN) coordinate system (Chang et al., 2018), and subsequently to a global East-North-Up (ENU) coordinate system (Brouwer and Hanssen, 2024).

The method assumes that deformation within each region of uniform motion (RUM), defined here as a 450×450 m area, is spatially constant, i.e., all PS within the RUM share the same displacement behavior and average linear velocity. Second, as the TLN-frame is right-handed with the longitudinal direction tangential to the iso-displacement contours and the transversal direction defined positive down-slope, i.e., in the direction of increasing subsidence, it assumes that all transversal estimates are positive.

The initial TLN coordinate system orientation (Brouwer and Hanssen, 2024) is approximated using three angles: Λ, the azimuth of the longitudinal direction relative to geographic north, initialized by computing the 2D gradient of LoS velocities projected onto the vertical; Φ, the elevation angle of the longitudinal direction relative to the horizontal; and Ω, the elevation angle of the transversal direction. Based on Jakarta's relatively flat terrain, with topographic slopes less than 2° (Abidin et al., 2005), we assume $\Phi = \Omega = 0$. Conservative uncertainties of $\sigma_\Lambda = 10°$, and $\sigma_\Phi = \sigma_\Omega = 3°$ are assigned to account for potential imperfections in the TLN orientation, yielding quality metrics for the ENU displacement velocity estimates.

[3]International GNSS Service (IGS) reference frame aligned with ITRF2014.

2.3. Inter-track InSAR datum alignment

The strapdown method requires both contributing InSAR viewing geometries to be in the same datum, see App. A. Ideally, an inter-track datum connection should be performed using terrestrial control points observable from both viewing geometries. Since such control points are currently not available in the area of interest, we exploit the fact that a datum offset between the two viewing geometries would alter both the magnitude and the sign of the decomposed transversal, $\hat{d}_T$, and normal, $\hat{d}_N$, velocities, which produces implausible results, e.g., transversal velocities pointing upslope (i.e., negative) instead of downslope (i.e., in the direction of increasing subsidence), and normal velocities may appear positive (uplift) in a sinking region. Therefore, we introduce a physical constraint in the strapdown method enforcing that the transversal components remain positive centripetal, i.e., directed towards greater subsidence rates, and estimate the relative datum offset, $\Delta d^{\text{asc}}_{\text{LoS}}$, of the ascending track datum relative to the descending track datum by minimizing the number of RUMs with negative transversal velocity. This can be expressed as

$$\min_{\Delta d^{\text{asc}}_{\text{LoS}}} \sum_{i=1}^{n} \mathbb{1}\Big(\hat{d}_{T_i}(d^{\text{asc}}_{\text{LoS}_i} + \Delta d^{\text{asc}}_{\text{LoS}}, d^{\text{dsc}}_{\text{LoS}_i}) < 0\Big), \tag{1}$$

where, $i = 1, \ldots, n$ indexes the n RUMs, and $\mathbb{1}(\cdot)$ is the indicator function, which equals 1 if the argument is true (i.e., if the transversal velocity is pointing downslope, hence positive) and 0 otherwise.

This optimization is achieved via an iterative search. The method is independent of the choice of reference track, and the alignment is always performed to a common InSAR datum, which may be defined using the datum of either track. In this study, we select the descending track as the common InSAR datum and align the ascending track with respect to it.

A bias offset is incrementally applied to the ascending-track LoS velocities in steps of 0.1 mm/yr, $d^{\text{asc}}_{\text{LoS}_i} + \Delta d^{\text{asc}}_{\text{LoS}}$, followed by the strapdown decomposition. The optimal offset, $\Delta \hat{d}^{\text{asc}}_{\text{LoS}}$, is identified as the value that best satisfies the minimum condition, see Eq. (1). Applying the estimated offset $\Delta \hat{d}^{\text{asc}}_{\text{LoS}}$ to the ascending track LoS velocities and performing the strapdown decomposition yields the unbiased normal and transversal velocity components $\hat{d}_{N_i}, \hat{d}_{T_i}$ for all RUMs, and subsequently their ENU displacement velocity estimates and variance-covariance matrices, in the local datum of the descending InSAR viewing direction.

2.4. InSAR and GNSS datum alignment

Since the estimated ENU displacement velocities are now given in the datum of the descending InSAR track, they need to be expressed in a terrestrial reference frame to facilitate meaningful geophysical interpretation. We chose to express the InSAR velocities of each RUM in the Sunda plate-fixed frame (Bock et al., 2003). Thus, the 3D motion of the local descending InSAR (dI) datum relative to the Sunda plate-fixed frame (S) must be estimated. This can be accomplished by comparing GNSS-derived 3D velocities in the Sunda plate-fixed frame, denoted by $\hat{d}_i^{\mathrm{G|S}}$, with InSAR-derived velocity estimates in the local descending InSAR datum, denoted by $\hat{d}_i^{\mathrm{I|dI}}$, at one or more co-located sites within RUM footprints of 450×450 m, see Fig. 3,

$$\Delta d^{\mathrm{dI}\to\mathrm{S}} = \hat{d}_i^{\mathrm{G|S}} - \hat{d}_i^{\mathrm{I|dI}}, \tag{2}$$

where $\Delta d^{\mathrm{dI}\to\mathrm{S}}$ is the datum connection vector. This datum offset can subse-

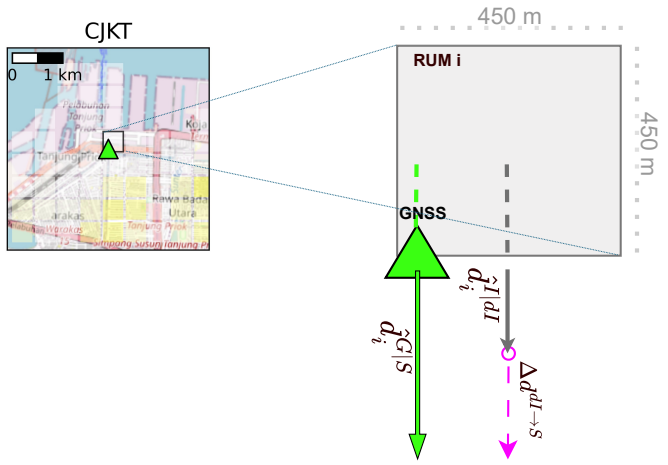

Figure 3: Estimation of InSAR velocities in the Sunda plate-fixed frame using GNSS. Left: Area containing GNSS benchmark at station CJKT (green triangle); the corresponding 450 × 450 m RUM is outlined in black. Right: Zoom at the RUM level (450 × 450 m footprint), where the InSAR RUM velocity in the local descending InSAR datum, $\hat{d}_i^{\mathrm{I|dI}}$ (grey arrow), is compared with the GNSS velocity in the Sunda plate-fixed frame, $\hat{d}_i^{\mathrm{G|S}}$ (green arrow). Their difference yields the datum-connection vector, $\Delta d^{\mathrm{dI}\to\mathrm{S}}$ (magenta dashed arrow), which links the InSAR velocities to the Sunda plate-fixed frame, see Eq. (2).

quently be applied uniformly to the relative InSAR velocity field to obtain the velocities in the Sunda plate-fixed frame:

$$\hat{d}_i^{\mathrm{I|S}} = \hat{d}_i^{\mathrm{I|dI}} + \Delta d^{\mathrm{dI}\to\mathrm{S}}. \tag{3}$$

3. Results

To estimate unbiased three-dimensional land motion in Jakarta with associated uncertainties, we first align the ascending-track datum to the descending-track datum, establishing a common InSAR datum shared by both tracks. Following the procedure described in Sec. 2.3, we estimate a relative datum offset of $\Delta\hat{d}^{\mathrm{asc}}_{\mathrm{LoS}} = 1.2$ mm/yr for the ascending track. During the iterations, the number of RUMs with negative transversal velocities decreases until convergence is reached (see animation in Sup. `figures/rum_bias_animation_sup1.gif`). Subsequently, the strapdown decomposition yields a first relative velocity map of Jakarta, see Fig. 4. The map shows vertical velocities in color, and directional horizontal velocities with vectors. Only vectors with magnitudes greater than 2σ are plotted, ensuring a confidence level of at least 95% that they represent genuine signals rather than noise. Subsidence bowls are clearly visible.

We connect this intermediary velocity map to the Sunda plate-fixed frame, as discussed in Sec. 2.4. This connection is applied in the vertical dimension only, see Eq. (3), using the vertical velocity of the CJKT GNSS station antenna over the InSAR observation period. CJKT shows a vertical velocity of -4.6 ± 0.2 mm/yr for 2014–2022, providing an independent estimate of $\Delta d^{\mathrm{dI}\to\mathrm{S}} = 0.2 \pm 0.2$ mm/yr, see Eq. (2). We adopt this value as the datum connection vector between the descending InSAR datum and the Sunda plate-fixed frame.

3.1. Application of the datum offset

Applying the CORS-based datum offset, see Eq. (3), of 0.2 ± 0.2 mm/yr to the vertical velocities of all RUMs produces the Sunda plate-fixed velocity map shown in Fig. 5. Horizontal velocities along the rims of the major subsidence bowls (outlined and numbered in turquoise in Fig. 5) exceed 10 mm/yr, including distinct north components. The estimation of north motion is particularly significant, as conventional East–Up decompositions typically neglect this component (Harintaka et al., 2024). These centimeter-level horizontal velocities indicate substantial lateral ground movement, with direct implications for the stability of buildings, utilities, and buried infrastructure.

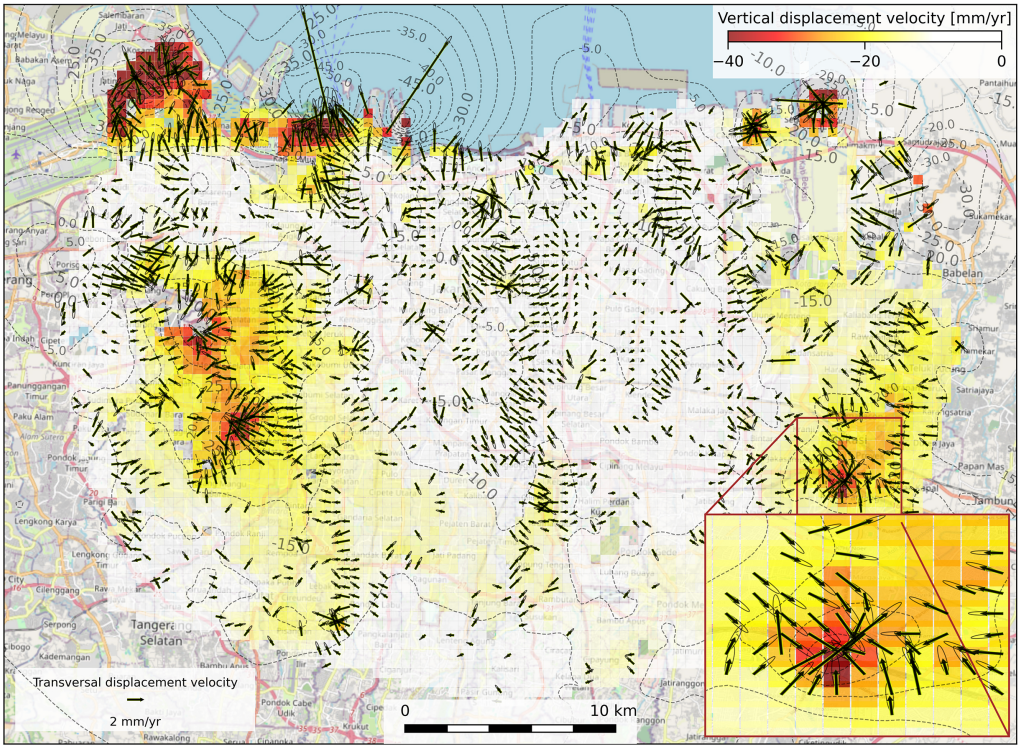

Figure 4: Relative 3D InSAR velocity map of the Jakarta metropolitan area over the Sentinel-1 observation period (2014–2025). Vertical velocities are shown in color, and directional horizontal velocities are shown as vectors, with associated 2σ confidence ellipses. Vectors are only depicted if their magnitude exceeds 2σ. Subsidence bowls are clearly visible. The map remains relative, since the unknown motion of the descending InSAR datum is not yet corrected; i.e., all velocities are still in the local InSAR datum.

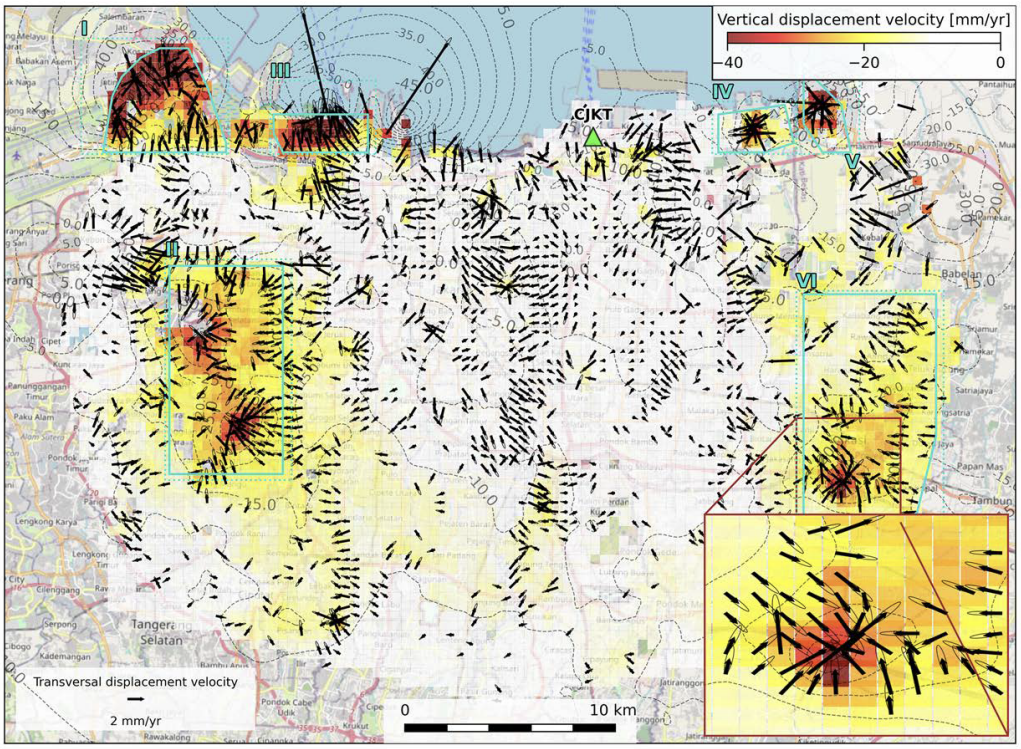

Figure 5: Sunda plate-fixed InSAR velocity map of the Jakarta metropolitan area (2014–2025) obtained via the single-station GNSS (green triangle) based datum connection. Vertical velocities are shown in color, and horizontal velocities are shown as vectors with 2σ confidence ellipses; only vectors exceeding 2σ are displayed. Six subsidence bowls (I–VI) are outlined in turquoise. Horizontal velocities near the bowl rims reach up to 10 mm/yr, including distinct north components. Central Jakarta shows little subsidence. The map closely matches Fig. 4, with only minor differences in the vertical dimension, indicating an overall mean subsidence rate exceeding -1.1 mm/yr across the Jakarta region.

4. Discussion

4.1. Geodetic discussion

Even millimeter-scale misalignments between InSAR LoS datasets from different tracks can propagate through the strapdown decomposition and distort the estimated velocity components. A sensitivity analysis for Jakarta, see App. A, shows that neglected inter-track datum offsets in the strapdown method may produce biases in both the magnitude and direction (sign flip) of the transversal velocities, whereas normal velocities are affected only about one quarter as much in magnitude and roughly one tenth as much in direction compared to transversal velocities. To minimize these biases from the earliest stage of the decomposition, we firstly align the tracks using the InSAR LoS data themselves rather than GNSS, as the dense and redundant InSAR sampling enables a more internally consistent track alignment. Relying on GNSS point measurements for this initial alignment would require the assumption that the CJKT GNSS-derived LoS velocity is representative of the spatially averaged InSAR motion in its vicinity—an assumption that is not guaranteed in the absence of in situ geometric ties between the GNSS and InSAR datasets. Applying this assumption at the pre-decomposition stage could introduce millimeter-scale inter-track datum misalignments, which would propagate through the strapdown method and have far larger impacts on the resulting 3D velocity estimates. We therefore rely on this assumption only later for the final connection to the Sunda plate-fixed frame.

The success of the strapdown decomposition in Jakarta relies on the way in which deformation is distributed within the subsidence bowl regions. These regions show smooth changes in velocity along the iso-deformation lines and strong radial gradients. These features create a continuous and well-defined approximate orientation of the local TLN coordinate system, enabling the full reconstruction of the 3D displacement velocity field.

By aligning the strapdown-derived 3D velocity field in Fig. 4 to the Sunda plate-fixed frame using the GNSS dataset, we obtain the 3D velocity map shown in Fig. 5. While the difference between the results before and after the datum connection is small (0.2 ± 0.2 mm/yr) in the current case study, this cannot be considered a given for other situations. Particularly in complex and dynamic settings, finding an area with known subsidence rates is not always possible, and at the very least, may be subject to discussion.

4.2. Geophysical discussion

The 3D velocity map in the Sunda plate-fixed frame reveals six spatially localized subsidence bowls, labeled I to VI in Fig. 5 and outlined in turquoise. These bowls exhibit maximum vertical velocities of up to −78.5 mm/yr, and their subsidence characteristics are summarized in Tab. 1. Bowl III in

Bowl #	**# RUMs**	$\hat{d}_{U_i}$ [mm/yr]			$\hat{d}_{T_i}$ [mm/yr]		
		mean	**max**	**max cum. [mm]**	**mean**	**max**	**max cum. [mm]**
I	112	−31.1	−55.9	−594.9	1.5	6.6	69.6
II	275	−21.9	−39.8	−423.4	1.0	3.8	40.4
III	44	−29.7	−78.5	−835.3	2.4	16.9	179.5
IV	32	−15.6	−35.1	−373.9	1.1	4.8	51.1
V	22	−26.0	−51.0	−542.6	2.1	9.8	104.0
VI	358	−17.1	−47.0	−500.2	0.7	5.8	61.7

Table 1: Summary of mean and maximum vertical and transversal subsidence rates and cumulative displacements in Jakarta for each subsidence bowl, based on the CORS-based datum alignment. Velocities are in mm/yr, and cumulative displacements cover a 10.7-year period (October 2014 to June 2025) in mm.

the Muara Angke region shows the strongest deformation, with vertical velocities up to −78.5 mm/yr, a cumulative vertical displacement of −84 cm over the October 2014–June 2025 period, and directional horizontal velocities up to 16.9 mm/yr that may pose risks to utility infrastructure. Bowl I, near Soekarno–Hatta International Airport, also exhibits severe vertical subsidence (maximum −55.9 mm/yr; cumulative −59 cm). The remaining four bowls show substantial but less extreme deformation. In addition to these localized zones of extreme sinking, the entire metropolitan area experiences a slow, regional subsidence, with a mean vertical velocity of −11.2 mm/yr across the Jakarta region.

To estimate these subsidence rates in the Sunda plate-fixed frame, we rely on the GNSS time series of CJKT, the only CORS station in Jakarta that spans the period 2014–2022. This dataset results from the direct processing of raw RINEX data (Susilo et al., 2023) and provides a precise and highly redundant vertical velocity estimate, making it preferable over other campaign-style GNSS datasets (Abidin et al., 2008) that are temporally sparse[4] and

[4]surveys conducted roughly every 2 years and 10 months (Abidin et al., 2008)

lack detailed documentation of processing methods, which prevents rigorous scrutiny. However, using a single GNSS site for the connection to the Sunda plate-fixed frame introduces limitations. As CJKT is installed on a tall building, likely supported by a deep-pile foundation, its motion may not fully represent the average ground movement of the surrounding RUM, as it misses potential compactions of shallower layers. This limitation is related to the assumption made in the first stage of our discussion, that InSAR vertical velocities averaged over 450×450 m RUM patches are physically comparable to co-located GNSS velocities. In heterogeneous urban environments, this assumption may not always hold, and applying it at the final connection stage could result in underestimation of vertical velocities and cumulative displacements. For example, Sidiq et al. (2025) report maximum rates up to −100 mm/yr, roughly 28% higher than the more conservative maximum vertical velocity in Tab. 1.

Given these constraints, the geophysical assessment of Jakarta's subsidence hinges on the presented single CORS-based datum connection. To improve future monitoring and enable rigorous alignment between InSAR and GNSS observations, new monitoring infrastructure is urgently needed in Jakarta. Establishing multiple Integrated Geodetic Reference Stations (IGRS) (Hanssen, 2017), which combine GNSS and corner reflectors and are visible in multiple InSAR viewing geometries, would facilitate precise geometric ties between InSAR and GNSS and ensure a rigorous alignment of the InSAR datum to the Sunda plate-fixed frame.

5. Conclusion

Three-dimensional displacement velocities are estimated for Jakarta for a grid of 450 × 450 m resolution cells, covering the time period 2014–2025, and referenced to the Sunda plate-fixed frame. All estimates are accompanied by a full variance–covariance matrix, enabling the detailed analysis of the significance and importance of the displacements, e.g., for city planning and asset management purposes. This 3D velocity field reveals that Jakarta's land motion is dominated by a superposition of six distinct subsidence bowls reflecting extreme localized deformation (maximum vertical velocity −77.4 mm/yr), superimposed on a slow, regional subsidence with an average vertical velocity of −11.2 mm/yr across the metropolitan area. Localized directional horizontal displacements of up to 17 mm/yr are observed and are statistically significant.

Currently, the connection of the InSAR velocity field to the Sunda plate-fixed frame hinges on a single long-term CORS GNSS station in Jakarta, and on the assumption that its velocity is representative of the surrounding region of uniform motion. While this enables a first-order plate-fixed alignment, it may underestimate the magnitude of vertical velocities and cumulative displacements. Addressing this limitation will require establishing additional monitoring infrastructure that facilitates direct InSAR–GNSS geometric ties, ensuring rigorous datum alignment and accurate assessment of the land subsidence threatening Jakarta's long-term coastal and urban resilience.

The findings result from a novel procedure, combining the strapdown decomposition on ascending and descending InSAR displacement velocity estimates, a data-based internal datum connection based on magnitude and directional constraints, and a global datum connection to a terrestrial reference frame using the GNSS–InSAR alignment.

This procedure can be considered as a generic and transferable framework for estimating 3D land motion in other rapidly sinking megacities, demonstrating that careful InSAR datum alignment is as critical as the subsidence measurements themselves.

Supplementary material

Supplementary material is available for this article. The following appendices provide additional detail supporting the main text, including supplementary conceptual illustrations and extended results presented as figures. A supplementary animation is also included, showing the iterative procedure for estimating the inter-track datum offset, $\Delta\hat{d}^{\mathrm{asc}}_{\mathrm{LoS}}$, described in Sec. 2.3. All supplementary materials should be treated as supporting information to the main article.

Acknowledgements

We thank Dr. F. van Leijen for valuable input on selecting InSAR processing parameters in DePSI. We also thank Bayu Triyogo Widyantoro, Sidik Tri Wibowo, and Febrylian Fahmi Chabibi from Badan Informasi Geospasial (BIG) for providing the GNSS data of the CORS station at CJKT in RINEX format.

Funding

This work was supported by the Dutch Research Council (NWO) through the Three SISTERS (grant no: NWO-WOTRO-482.21.505) project and by the Merian Fund Southeast Asia–Europe Joint Funding Scheme.

Declaration of Competing Interest

The authors declare that they have no known competing financial interests or personal relationships that could have appeared to influence the work reported in this paper.

Data availability

The final 3D ground displacement velocity estimates (east, north, up) for the Jakarta city and metropolitan area, including variance-covariance values are available at `https://doi.org/10.4121/39e7a39c-d305-425f-b238-1f3a4271dda9`. The North–East–Up GNSS time series of the CJKT CORS station are available from the Zenodo repository at `https://doi.org/10.5281/zenodo.7775016` (Susilo et al., 2023).

All other data and materials required to evaluate the conclusions of this study are included in the article and the supplementary material.

Author Contributions

A.M.L. contributed to Conceptualization, Methodology, Formal analysis, Investigation, Data Curation, Visualization, and Writing – Original Draft; designed the research, performed the analysis, created the figures, and wrote the first draft. H.A. contributed to Investigation, Resources, Data Curation, and Writing – Review & Editing; conducted, processed, and provided the GNSS data and additional metadata on the GNSS benchmarks. D.P. contributed to Investigation, Resources, and Data Curation; conducted, processed, and provided the GNSS data and additional metadata on the GNSS benchmarks. W.B. contributed to Methodology and Software; developed the strapdown method and provided feedback on its application. S.v.D. contributed to Investigation and Data Curation; processed the InSAR data. R.H. contributed to Supervision and Writing – Review & Editing; analyzed, reviewed, and edited the manuscript.

A. Effect of inter-track datum misalignment on the relative velocity map of Jakarta

To quantify the impact of datum misalignment on the decomposed 3D velocity field, we compute both magnitude and directional (sign flip) residuals between the unaligned ($\Delta d^{\mathrm{asc}}_{\mathrm{LoS}} = 0$ mm/yr) and aligned ($\Delta \hat{d}^{\mathrm{asc}}_{\mathrm{LoS}} = 1.2$ mm/yr) decomposed velocity fields of each RUM, after the inter-track datum alignment, see Sec. 2.3. Magnitude residuals are defined as:

$$\begin{aligned} \Delta \hat{d}_{T_i} &= \hat{d}_{T_i}\big(d^{\mathrm{asc}}_{\mathrm{LoS}_i}, d^{\mathrm{dsc}}_{\mathrm{LoS}_i}\big) - \hat{d}_{T_i}\big(d^{\mathrm{asc}}_{\mathrm{LoS}_i} + \Delta d^{\mathrm{asc}}_{\mathrm{LoS}_i}, d^{\mathrm{dsc}}_{\mathrm{LoS}_i}\big), \\ \Delta \hat{d}_{N_i} &= \hat{d}_{N_i}\big(d^{\mathrm{asc}}_{\mathrm{LoS}_i}, d^{\mathrm{dsc}}_{\mathrm{LoS}_i}\big) - \hat{d}_{N_i}\big(d^{\mathrm{asc}}_{\mathrm{LoS}_i} + \Delta d^{\mathrm{asc}}_{\mathrm{LoS}_i}, d^{\mathrm{dsc}}_{\mathrm{LoS}_i}\big). \end{aligned} \tag{A.1}$$

The magnitude bias is expressed as the Weighted Mean Absolute Bias (WMAB):

$$\begin{aligned} \mathrm{WMAB}_T &= \frac{1}{n}\sum_{i=1}^{n} \big|\Delta \hat{d}_{T_i}\big|, \\ \mathrm{WMAB}_N &= \frac{1}{n}\sum_{i=1}^{n} \big|\Delta \hat{d}_{N_i}\big|. \end{aligned} \tag{A.2}$$

Directional (sign flip) bias is measured as the percentage of RUMs exhibiting a polarity flip:

$$\begin{aligned} \Delta\theta_T &= \frac{100}{n}\sum_{i=1}^{n} \mathbb{1}\Big(\hat{d}_{T_i}\big(d^{\mathrm{asc}}_{\mathrm{LoS}_i}, d^{\mathrm{dsc}}_{\mathrm{LoS}_i}\big) \cdot \hat{d}_{T_i}\big(d^{\mathrm{asc}}_{\mathrm{LoS}_i} + \Delta d^{\mathrm{asc}}_{\mathrm{LoS}_i}, d^{\mathrm{dsc}}_{\mathrm{LoS}_i}\big) < 0\Big), \\ \Delta\theta_N &= \frac{100}{n}\sum_{i=1}^{n} \mathbb{1}\Big(\hat{d}_{N_i}\big(d^{\mathrm{asc}}_{\mathrm{LoS}_i}, d^{\mathrm{dsc}}_{\mathrm{LoS}_i}\big) \cdot \hat{d}_{N_i}\big(d^{\mathrm{asc}}_{\mathrm{LoS}_i} + \Delta d^{\mathrm{asc}}_{\mathrm{LoS}_i}, d^{\mathrm{dsc}}_{\mathrm{LoS}_i}\big) < 0\Big), \end{aligned} \tag{A.3}$$

where $\mathbb{1}(\cdot)$ is the indicator function, which equals 1 if the argument is true (i.e., if the unaligned decomposed velocity has the opposite sign to the aligned decomposed velocity for the same RUM, their product will be negative) and 0 otherwise. For transversal velocities, the positive direction is defined as downslope (centripetal), while normal velocities are expected to be negative in sinking regions.

Fig. A.6 compares the unaligned and aligned decomposed velocities over the entire RUM field. Transversal velocities show a magnitude bias of $\mathrm{WMAB}_T = 6.86$ mm/yr and directional flips $\Delta\theta_T = 33\%$, whereas normal velocities show smaller biases: $\mathrm{WMAB}_N = 1.51$ mm/yr and $\Delta\theta_N = 2\%$.

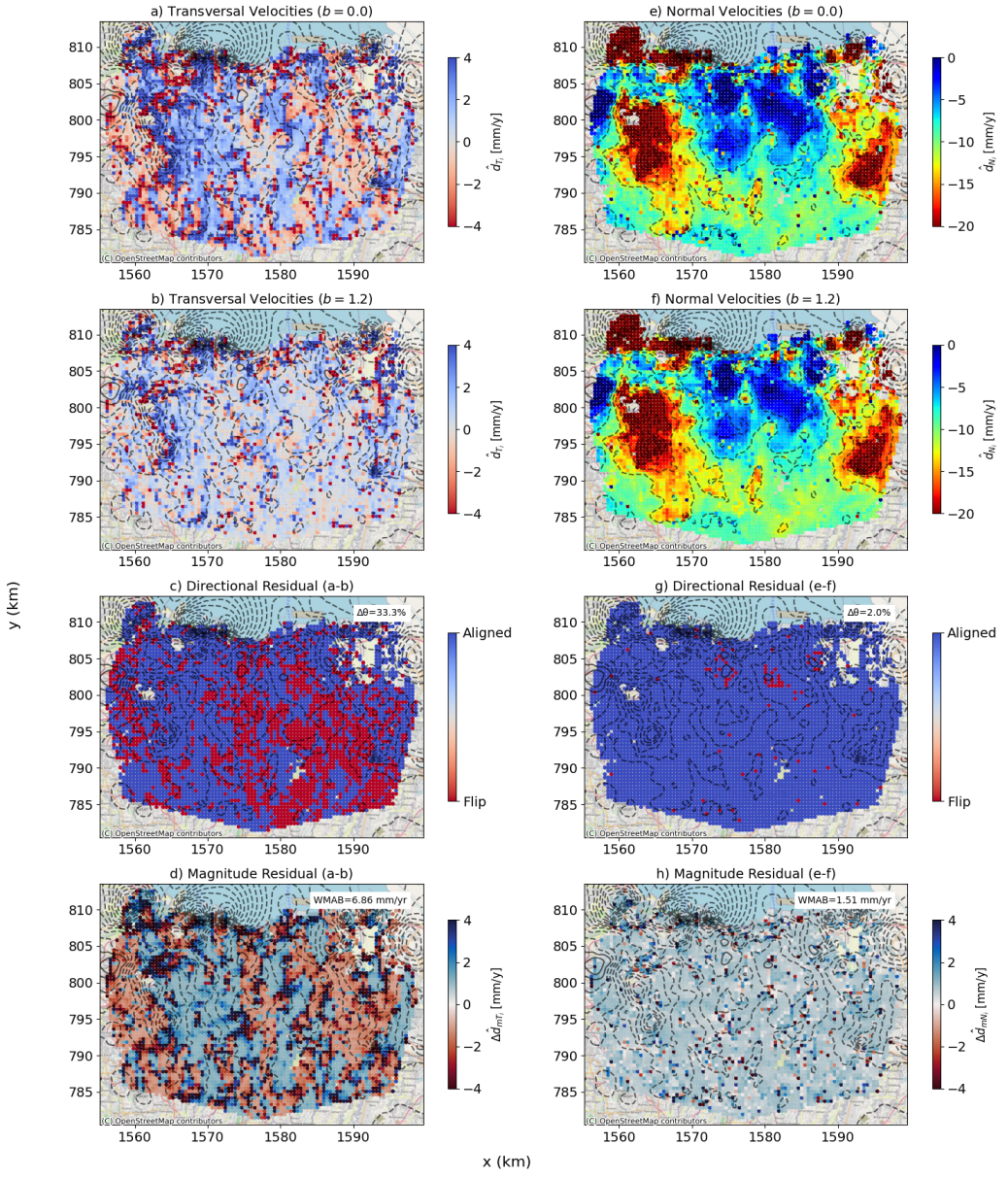

Figure A.6: Directional and magnitude biases due to inter-track datum misalignment in Jakarta. Columns show transversal (first) and normal (second) velocity components. Panels (a)–(b) compare unaligned ($\Delta d^{\text{asc}}_{\text{LoS}} = 0.0\,\text{mm/yr}$) and aligned ($\Delta d^{\text{asc}}_{\text{LoS}} = 1.2\,\text{mm/yr}$) transversal velocities; panels (e)–(f) show the same for normal velocities. Panels (c)–(d) and (g)–(h) display spatial variability of directional and magnitude biases.

Fig. A.7 shows the effect of varying the ascending track datum offset, $\Delta d_{\mathrm{LoS}}^{\mathrm{asc}}$, from -2.2 to $+2.2$ mm/yr in steps of 0.1 mm/yr. Transversal velocities reach up to 20 mm/yr (WMAB) and 45% directional flips, while normal velocities reach up to 4.8 mm/yr and 5% flips. Both magnitude and directional biases show a clear minimum at $\Delta d_{\mathrm{LoS}}^{\mathrm{asc}} = 1.2$ mm/yr, highlighting the necessity of proper datum alignment.

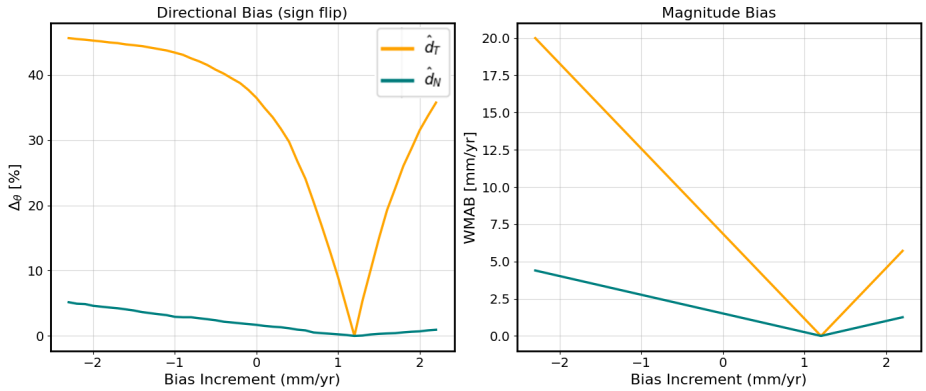

Figure A.7: Directional bias ($\Delta\theta$, left) and magnitude bias (WMAB, right) for transversal (T, orange) and normal (N, blue) velocity components across inter-track datum offsets. Transversal velocities are more sensitive, reaching 20 mm/yr (WMAB) and 45% ($\Delta\theta$). Both curves show a minimum at $\Delta d_{\mathrm{LoS}}^{\mathrm{asc}} = 1.2$ mm/yr.

References

Abdullah, F.M., Andriyanto, H., Nababan, J.R., Abdillah, F., Sulistyawan, R.I.H., 2021. Results of Land Subsidence Measurement using GPS Method in the Jakarta Groundwater Basin in 2015–2019, in: IOP Conference Series: Earth and Environmental Science, p. 012034. doi:https://doi.org/10.1088/1755-1315/873/1/012034.

Abidin, H., Djaja, R., Andreas, H., Gamal, M., Hirose, K., Maruyama, Y., 2004. Capabilities and Constraints of Geodetic Techniques for Monitoring Land Subsidence in the Urban Areas of Indonesia. Geomatics Research Australia 81, 45–58.

Abidin, H.Z., Andreas, H., Djaja, R., Darmawan, D., Gamal, M., 2008. Land Subsidence Characteristics of Jakarta between 1997 and 2005, as estimated using GPS Surveys. GPS Solutions 12, 23–32. doi:https://doi.org/10.1007/s10291-007-0061-0.

Abidin, H.Z., Andreas, H., Gamal, M., Djaja, R., Subarya, C., Hirose, K., Maruyama, Y., Murdohardono, D., Rajiyowiryono, H., 2005. Monitoring Land Subsidence of Jakarta (Indonesia) using Leveling, GPS Survey and InSAR Techniques, in: A Window on the Future of Geodesy: Proceedings of the International Association of Geodesy IAG General Assembly, Sapporo, Japan, June 30–July 11, 2003, pp. 561–566. doi:https://doi.org/10.1007/3-540-27432-4_95.

Abidin, H.Z., Andreas, H., Gumilar, I., Brinkman, J.J., 2015. Study on the Risk and Impacts of Land Subsidence in Jakarta. Proceedings of the International Association of Hydrological Sciences 372, 115–120. doi:https://doi.org/10.5194/piahs-372-115-2015.

Abidin, H.Z., Andreas, H., Gumilar, I., Fukuda, Y., Pohan, Y.E., Deguchi, T., 2011. Land Subsidence of Jakarta (Indonesia) and its Relation with Urban Development. Natural Hazards 59, 1753–1771. doi:https://doi.org/10.1007/s11069-011-9866-9.

Abidin, H.Z., Andreas, H., Gumilar, I., Sidiq, T.P., Pradipta, D., Yuwono, B.D., 2022. On the Disaster Risk Reduction of Land Subsidence in Indonesia's Northern Coastal Areas of Java, in: EGU General Assembly Conference Abstracts, pp. EGU22–1721. doi:https://doi.org/10.13140/RG.2.2.34300.00646.

Abidin, H.Z., Djaja, R., Darmawan, D., Hadi, S., Akbar, A., Rajiyowiryono, H., Sudibyo, Y., Meilano, I., Kasuma, M.A., Kahar, J., 2001. Land Subsidence of Jakarta (Indonesia) and its Geodetic Monitoring System. Natural Hazards 23, 365–387.

Batubara, B., Kooy, M., Zwarteveen, M., 2023. Politicising Land Subsidence in Jakarta: How Land Subsidence is the Outcome of uneven Sociospatial and Socionatural Processes of Capitalist Urbanization. Geoforum 139, 1–9.

Bennett, W.G., Karunarathna, H., Xuan, Y., Kusuma, M.S., Farid, M., Kuntoro, A.A., Rahayu, H.P., Kombaitan, B., Septiadi, D., Kesuma, T.N., et al., 2023. Modelling Compound Flooding: A Case Study from Jakarta, Indonesia. Natural Hazards 118, 277–305. doi:https://doi.org/10.1007/s11069-023-06001-1.

Berardino, P., Fornaro, G., Lanari, R., Sansosti, E., 2003. A new Algorithm for Surface Deformation Monitoring based on Small Baseline Differential SAR Interferograms. IEEE Transactions on Geoscience and Remote Sensing 40, 2375–2383. doi:https://doi.org/10.1109/TGRS.2002.803792.

Bock, Y., Prawirodirdjo, L., Genrich, J.F., Stevens, C.W., McCaffrey, R., Subarya, C., Puntodewo, S.S.O., Calais, E., 2003. Crustal Motion in Indonesia from Global Positioning System Measurements. Journal of Geophysical Research: Solid Earth 108. doi:https://doi.org/10.1029/2001JB000324.

Brouwer, W.S., Hanssen, R.F., 2021. An Analysis of InSAR Displacement Vector Decomposition Fallacies and the Strap-Down Solution, in: 2021 IEEE International Geoscience and Remote Sensing Symposium (IGARSS), pp. 2927–2930.

Brouwer, W.S., Hanssen, R.F., 2023. A Treatise on InSAR Geometry and 3-D Displacement Estimation. IEEE Transactions on Geoscience and Remote Sensing 61, 1–11. doi:https://doi.org/10.1109/TGRS.2023.3322595.

Brouwer, W.S., Hanssen, R.F., 2024. Estimating Three-Dimensional Displacements with InSAR: The Strapdown Approach. Journal of Geodesy 98, 110.

Chang, L., Dollevoet, R.P., Hanssen, R.F., 2018. Monitoring line-infrastructure with multisensor sar interferometry: products and performance assessment metrics. IEEE journal of selected topics in applied earth observations and remote sensing 11, 1593–1605.

Chaussard, E., Amelung, F., Abidin, H., Hong, S.H., 2013. Sinking Cities in Indonesia: ALOS PALSAR detects rapid Subsidence due to Groundwater and Gas Extraction. Remote Sensing of Environment 128, 150–161. doi:https://doi.org/10.1016/j.rse.2012.10.015.

Colbran, N., 2009. Will Jakarta be the next Atlantis? Excessive Groundwater Use resulting from a Failing Piped Water Network. Law, Environment and Development Journal 5, 18. URL: http://www.lead-journal.org/content/09018.pdf.

Ekkelenkamp, H., 2019. Indonesië op de Kaart: De Rol van de Nederlandse Aanwezigheid in Indonesië bij de Ontwikkeling van de Geodesie in Nederland .

Fenoglio-Marc, L., Schöne, T., Illigner, J., Becker, M., Manurung, P., Khafid, 2012. Sea Level Change and Vertical Motion from Satellite Altimetry, Tide Gauges and GPS in the Indonesian Region. Marine Geodesy 35, 137–150. doi:https://doi.org/10.1080/01490419.2012.674063.

Ferretti, A., Prati, C., Rocca, F., 2002a. Nonlinear Subsidence Rate Estimation using Permanent Scatterers in Differential SAR Interferometry. IEEE Transactions on Geoscience and Remote Sensing 38, 2202–2212. doi:https://doi.org/10.1109/36.868878.

Ferretti, A., Prati, C., Rocca, F., 2002b. Permanent Scatterers in SAR Interferometry. IEEE Transactions on Geoscience and Remote Sensing 39, 8–20. doi:https://doi.org/10.1109/36.898661.

Firman, T., Surbakti, I.M., Idroes, I.C., Simarmata, H.A., 2011. Potential Climate-Change related Vulnerabilities in Jakarta: Challenges and current Status. Habitat International 35, 372–378. doi:https://doi.org/10.1016/j.habitatint.2010.11.011.

Hakim, W.L., Achmad, A.R., Eom, J., Lee, C.W., 2020. Land Subsidence Measurement of Jakarta Coastal Area using Time Series Interferometry

with Sentinel-1 SAR Data. Journal of Coastal Research 102, 75–81. doi:https://doi.org/10.2112/SI102-010.1.

Hanssen, R.F., 2001. Radar Interferometry: Data Interpretation and Error Analysis. Springer. doi:https://doi.org/10.1007/0-306-47633-9_4.

Hanssen, R.F., 2017. A radar retroreflector device and a method of preparing a radar retroreflector device. URL: https://patentimages.storage.googleapis.com/fe/ad/46/df362a63c8ed57/WO2018236215A1.pdf. patent WO 2018/236215 Al.

Harintaka, H., Suhadha, A.G., Syetiawan, A., Ardha, M., Rarasati, A., 2024. Current Land Subsidence in Jakarta: A multi-track SBAS InSAR Analysis during 2017–2022 using C-band SAR Data. Geocarto International 39, 2364726. doi:https://doi.org/10.1080/10106049.2024.2364726.

Herring, T.A., King, R.W., McClusky, S.C., et al., 2010. Introduction to GAMIT/GLOBK. Massachusetts Institute of Technology, Cambridge, Massachusetts 400, 401.

Hooper, A., 2008. A multi-temporal InSAR Method incorporating both Persistent Scatterer and Small Baseline Approaches. Geophysical Research Letters 35. doi:https://doi.org/10.1029/2008GL034654.

Hu, F., Wu, J., Chang, L., Hanssen, R.F., 2019. Incorporating temporary coherent scatterers in multi-temporal insar using adaptive temporal subsets. IEEE transactions on geoscience and remote sensing 57, 7658–7670.

Juliandri, F., Andreas, H., Pradipta, D., 2022. Efek Akurasi dan Geometrik Sistem Tinggi Digital Elevation Model (DEM) terhadap Pemodelan Banjir Rob di Jakarta. Bulletin of Geology 6, 934–948.

Kampes, B.M., 2006. Radar Interferometry: Persistent Scatterer Technique. Springer, Berlin.

Koudogbo, F.N., Duro, J., Arnaud, A., Bally, P., Abidin, H.Z., Andreas, H., 2012. Combined X- and L-Band PSI Analyses for Assessment of Land Subsidence in Jakarta, in: Remote Sensing for Agriculture, Ecosystems, and Hydrology XIV, pp. 46–58. doi:https://doi.org/10.1117/12.974821.

Lubis, S.W., Hagos, S., Hermawan, E., Respati, M.R., Ridho, A., Risyanto, Paski, J.A., Muhammad, F.R., Siswanto, Ratri, D.N., et al., 2022. Record-Breaking Precipitation in Indonesia's Capital of Jakarta in early January 2020 linked to the Northerly Surge, Equatorial Waves, and MJO. Geophysical Research Letters 49, e2022GL101513. doi:https://doi.org/10.1029/2022GL101513.

Murdohardono, D., Sudarsono, U., 1998. Land Subsidence Monitoring System in Jakarta, in: Proceedings of Symposium on Japan-Indonesia IDNDR Project: Volcanology, Tectonics, Flood and Sediment Hazards, pp. 243–256.

Ng, A.H.M., Ge, L., Li, X., Abidin, H.Z., Andreas, H., Zhang, K., 2012. Mapping Land Subsidence in Jakarta, Indonesia using Persistent Scatterer Interferometry (PSI) Technique with ALOS PALSAR. International Journal of Applied Earth Observation and Geoinformation 18, 232–242. doi:https://doi.org/10.1016/j.jag.2012.01.018.

Nugraha, G.U., Bakti, H., Lubis, R.F., Nur, A.A., 2024. Jakarta Groundwater Modeling: A Review. Applied Water Science 14, 186.

Sagala, S., Lassa, J., Yasaditama, H., Hudalah, D., 2013. The Evolution of Risk and Vulnerability in Greater Jakarta: Contesting Government Policy. Institute for Resource Governance and Social Change, Kupang, Indonesia .

Schepers, J., 1926. De Nauwkeurigheidswaterpassing van Java, de Primaire Kringen 1a en ii, benevens het Stadsnet van Batavia en Weltevreden. Verhandelingen No. 1, Topografische Dienst in Nederlandsch-Indië .

Schuitenvoerder, H., 1926. De Nauwkeurigheidswaterpassing van Java. Jaarverslag van den Topografischen Dienst in Nederlandsch-Indië 1925.

Sidiq, T.P., Gumilar, I., Abidin, H.Z., Meilano, I., Purwarianti, A., Lestari, R., 2025. Spatial Distribution and Monitoring of Land Subsidence using Sentinel-1 SAR Data in Java, Indonesia. Applied Sciences 15. doi:https://doi.org/10.3390/app15073732.

Susilo, S., Salman, R., Hermawan, W., Widyaningrum, R., Wibowo, S.T., Lumban-Gaol, Y.A., Meilano, I., Yun, S.H., 2023. GNSS Land Subsidence

Observations along the Northern Coastline of Java, Indonesia. Scientific Data 10, 421. doi:https://doi.org/10.1038/s41597-023-02274-0.

Takagi, H., Esteban, M., Mikami, T., Fujii, D., 2016. Projection of Coastal Floods in 2050 Jakarta. Urban Climate 17, 135–145. doi:https://doi.org/10.1016/j.uclim.2016.05.003.

United Nations, D.o.E., Social Affairs, P.D., 2025. World Urbanization Prospects 2025: Summary of Results. United Nations Department of Economic and Social Affairs, Population Division .

Van Leijen, F.J., 2014. Persistent Scatterer Interferometry Based on Geodetic Estimation Theory. Ph.D. thesis. Netherlands Geodetic Commission (NCG). Amersfoort, The Netherlands.

Widodo, J., Herlambang, A., Sulaiman, A., Razi, P., Perissin, D., Kuze, H., Sumantyo, J.T.S., 2019. Land Subsidence Rate Analysis of Jakarta Metropolitan Region based on D-InSAR Processing of Sentinel Data C-band Frequency, in: Journal of Physics: Conference Series, p. 012004. doi:https://doi.org/10.1088/1742-6596/1185/1/012004.

Yong, C.Z., Denys, P.H., Pearson, C.F., 2017. Present-day kinematics of the Sundaland plate. Journal of Applied Geodesy 11, 169–178. doi:10.1515/jag-2016-0024.

Zebker, H.A., Villasenor, J., 1992. Decorrelation in Interferometric Radar Echoes. IEEE Transactions on Geoscience and Remote Sensing 30, 950–959. doi:https://doi.org/10.1109/36.175330.

Zhang, J., Duan, W., Fu, X., Yun, Y., Lv, X., 2025. The stepwise multi-temporal Interferometric Synthetic Aperture Radar with partially Coherent Scatterers for long-time Series Deformation Monitoring. Remote Sensing 17, 1374. doi:https://doi.org/10.3390/rs17081374.